Rolfe and Rice 2019 Referee Edits

We would like to thank all of the reviewers for their thorough read of our manuscript and careful consideration of our study. In particular, we appreciate the point the reviewers make on comparison of our new dataset with N_2O and SF_6 datasets in the prior literature, technical questions, comments, and corrections to the work and in the text. We appreciate the technical corrections and believe this review process has helped to strengthen our manuscript.

Here we detail changes made in our revised manuscript in order to address particular points for Eric Ray.

Pg. 1, line 25: I think you mean 0.04 ppt rather than ppb.

We have revised the manuscript to correct this typographic error.

Pg. 3, line 19-20: There are two more recent studies on the lifetime of SF_6 that should be included here since they both significantly reduce the estimated lifetime, Ray et al., JGR, 2016 and Kovacs et al., ACP, 2017.

We have revised the manuscript to use updated estimates of the SF_6 lifetime from Kovacs et al (2017) and Ray et al. (2017) addressing this comment and that of reviewer #1.

Pg. 6, line 12: Change 'provides' to 'provide'.

We have revised the manuscript to correct this typographic error.

Pg. 7, line 21: Even though it's apparent from the values of the concentration you should add 'N_2O of' before '301.5' since the figure includes both N_2O and SF_6.

We have revised the manuscript to change language to "N_2O mixing ratio of…".

Section 3.1: You mention comparable measurements and their locations in the text of this section but it would be easier to see this information in a figure. What would be useful is a plot of concentration vs. latitude at two different times, one at the beginning of your measurement time series and one at the end. By including all available surface measurements, it will be easy to see how many other measurements exist for each time and how it changed. Since the concentrations changed enough over the period of your measurements you could just color the two different

times differently and they will fit on the same plot. The lack of measurements in the 1970s should be readily apparent from a plot of this type.

While we find adding raw data from prior studies makes Fig. 5 unnecessarily busy and detracts from this new contribution of Cape Meares data to the atmospheric community, we can see that a visual comparison of our results with prior work is useful in addition to the discussion we already have in the manuscript. Additionally, we note that much of the raw data for SF_6 previously published is not available through open access WDCGG (or other platforms). To address this, we have included a supplemental figure which compares regressed fits through the Cape Meares dataset with fits from other comparator sites in the literature. We hope this will help reader assess how this new dataset fits within historical published trends in N_2O and SF_6.

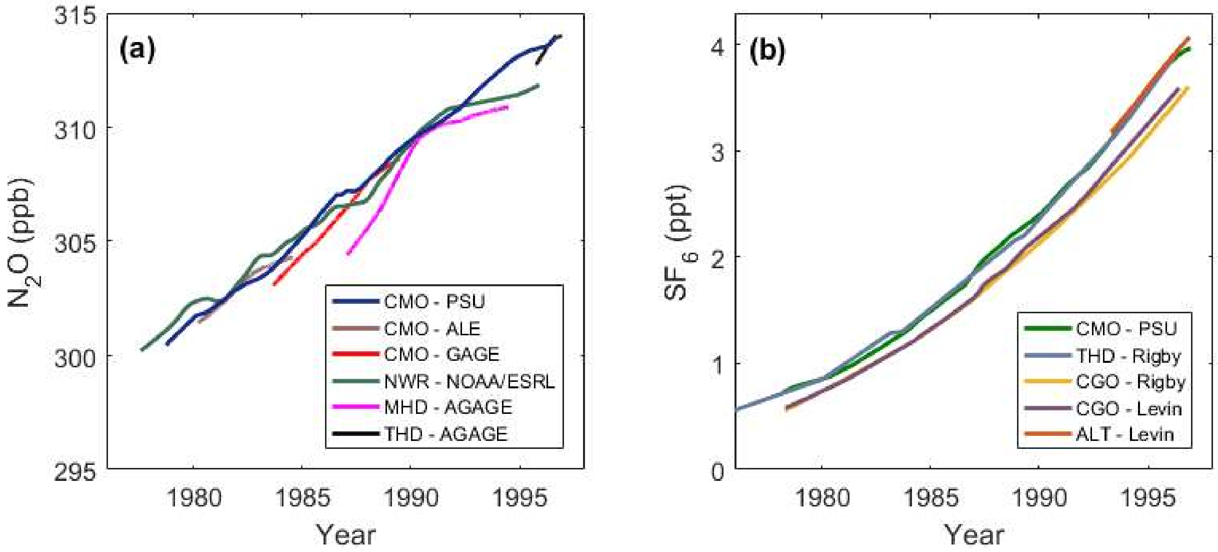

Figure S2. 3-year LOWESS regressions of measurements of mole fraction versus date of collection, N_2O (a) and SF_6 (b). Station codes: CMO = Cape Meares, Oregon, USA, NWR = Niwot Ridge, Colorado, USA, MHD = Mace Head, Ireland, THD = Trinidad Head, California, USA, CGO = Cape Grim, Tasmania, ALT = Alert, Canada. N_2O data sources: Atmospheric Lifetime Experiment (ALE, now AGAGE), Massachusetts Institute of Technology, Building 54-1312 Cambridge, MA 02139-2307, https://agage.mit.edu/; Global Atmospheric Gases Experiment (GAGE, now AGAGE), Massachusetts Institute of Technology, Building 54-1312 Cambridge, MA 02139-2307, https://agage.mit.edu/; National Oceanic and Atmospheric Association / Earth System Research Laboratory (NOAA/ESRL), 325 Broadway Boulder, CO 80305-3337, http://www.cmdl.noaa.gov/index.html; Advanced Global Atmospheric Gases Experiment Science Team (AGAGE), Massachusetts Institute of Technology, Building 54-1312 Cambridge, MA 02139-2307, https://agage.mit.edu/.

N_2O data collected from World Data Center for Greenhouse Gases (WDCGG) https://gaw.kishou.go.jp/. SF_6 data is digitized from plots in Rigby et al. 2010 and Levin et al. 2010.

Pg. 10, lines 23-25: Also, seasonal transport from the stratosphere can influence SF_6 due to the high growth rates, especially in these early years. Growth rates of ~10%/yr means that stratospheric air with a mean age of 2 years will have ~20% lower concentrations compared to tropospheric values. For example, the seasonal cycle of CFCs have a minimum in the summer of each hemisphere due to the transport of relatively low concentrations due to photochemical destruction (e.g. Liang et al., JGR, 2008).

We thank the reviewer for this valid point and have updated the final paragraph of section 3.3 to address it specifically:

> *Seasonal transport from STE adds relatively depleted SF_6 air into the troposphere from the stratosphere. The seasonal phase of SF_6 observed at Cape Meares closely reflects seasonality phasing observed in CFCs in the northern hemisphere driven by STE (Liang et al. 2008). Modeling atmospheric transport effects on SF_6 at Cape Meares could help confirm amplitude and phase reported here.*

Here we detail changes made in our revised manuscript in order to address particular points for Brad Hall.

Page 1, Line 17: Please consider using mixing ratio or mole fraction instead of concentration, or refer to "mole fraction in dry air" on first use of concentration. Concentration is the amount of substance in a defined space or volume.

We have updated the manuscript to use the more correct technical language and replaced concentration with mole fraction or mixing ratio throughout the document where appropriate.

Page 3, Line 20: Consider including recent papers that suggest a shorter lifetime for SF_6.

We have revised the manuscript to use updated estimates of the SF_6 lifetime from Kovacs et al. (2017) and Ray et al. (2017) addressing this comment and that of reviewer #1.

Page 4, Line 11: Is the air dried or collected wet?

We have added clarification here that air was dried upon collection, removing a significant amount of water vapor, using a condenser-type system.

Pg .3, Line 21: Seems like a more recent SF_6 mole fraction could be inserted here. Global mean mixing ratios are available from several sources, such as the AGAGE data repository (https://agage.mit.edu/data/agage-data) or State of the Climate reports: State of the Climate in 2017, supplement to the August 2017 issue of the Bulletin of the American Meteorological

We appreciate this point that the manuscript should use more updated SF_6 global mean mole fraction and used a recent calculation of 9.3ppt for the NH in January, 2017 from Prinn et al. (2018).

Page 5. Line 7: According to https://www.esrl.noaa.gov/gmd/ccl/refgas.html, the N2O scale associated with CB11406 (328.71 ppb) is NOAA-2006A (a 2011 update from NOAA-2006)

We have updated the manuscript to reflect this change.

Page 5, Line 13: Not sure what is meant by "sets of 6 gas analysis". Maybe just say "repeated analysis of a reference standard"?

We have updated the manuscript here for clarity changing the language to "determined by repeated analysis of the reference standard".

Page 6, line 11: Does the error stated here include the uncertainty on the SF_6 mole fraction in the dilution gas and SF_6 that might be present in the 1 ppm N_2O aliquot? 0.001 ppt seems too small, unless you have some other way to verify SF_6 in the dilution gas to better than 0.001 ppt.

This is an important point that the 0.001ppt error is from the uncertainty in manometric measurement alone. Both the dilution gas and the N_2O aliquot may have trace SF_6 at levels below the detection limits of our instrumentation and would also contribute to uncertainty in the resulting SF_6 prepared samples. We have updated this discussion to point out that uncertainty is larger when including this consideration.

> *The maximum error (1σ) in SF_6 introduced from the manometric process is small (0.001 ppt) compared to measurement uncertainty. However, SF_6 present in either ultra-pure air dilution gas or the N_2O aliquot at trace levels below the detection limit of our measurement (<0.1 ppt) contribute to the uncertainty in prepared samples.*

Page 6, Line 15: Shouldn't the slope, 0.870, be the inverse of the coefficient a1 (1.146)? These don't quite match.

We thank the reviewer for catching this technical error here. Indeed the slope should be the inverse of the coefficient a1. The equations have been updated to give the correct values.

Page 10, Line 7: check spelling of "Leuker" vs "Lueker" et al. (2003).

We have updated the manuscript to include this change.

Page 10, Line 23: Is it known that SF_6 sources are a-seasonal? Please provide a reference.

We have included a reference to a global CTM modeling study by Patra et al. (2009) which simulated SF_6 mixing ratios and their seasonality at remote sites using emissions inventory (EDGAR) that lack seasonality. Thus the simulation, which matches seasonality well for remote sites (only), appears driven primarily by atmospheric transport. Additionally, we have been unable to find a (bottom-up or top-down) SF_6 emissions inventory with a significant seasonality.

Here we detail changes made in our revised manuscript in order to address particular points for Andreas Engel.

Figure 1 isn't very nice and needs to be improved.

We do agree that the resolution in the schematic of our GC-ECD system was poor and have updated the figure output file to improve its resolution.

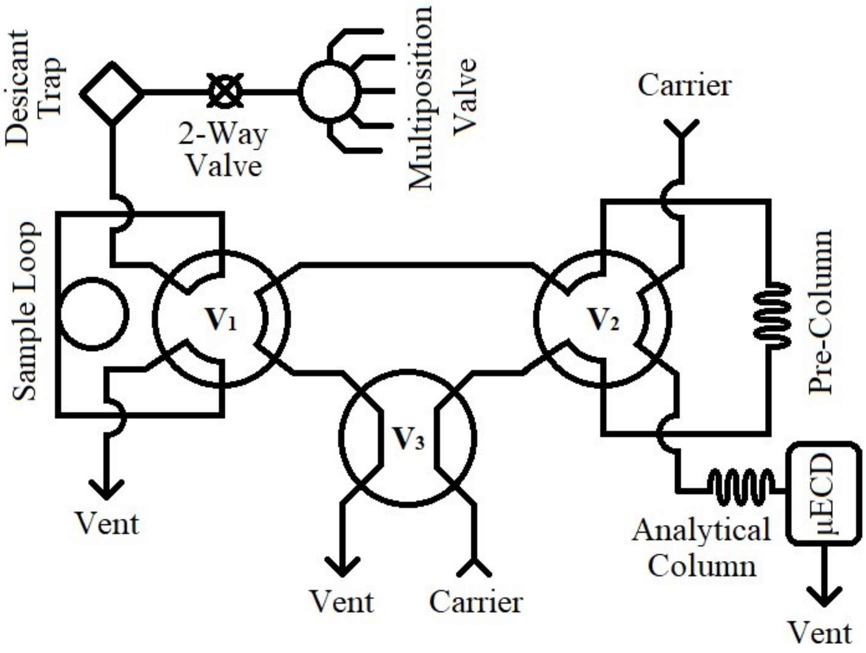

Replace Non-Linear plots with Difference plots.

We agree that difference plots can provide additional insight where non-linear effects are large. However, after consideration, we do feel that the measured v. expected plots shown in Fig. 4 are straightforward to interpret. For this reason, we have kept Fig. 4 as is and added additional difference plots for N_2O and SF_6 in the supplemental documentation over the entire range measured. We also refer to these plots within the text when discussing non-linear effects.

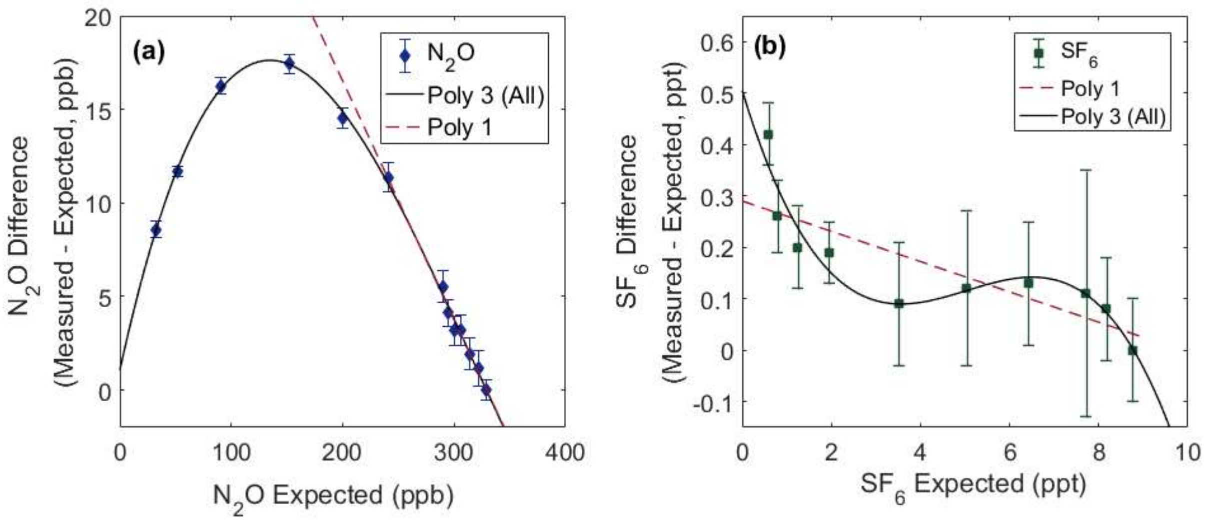

Figure S1. Mole fraction difference from expected plots for N_2O (a) and SF_6 (b) detector response calibration measurements. Solid black lines are 3rd-degree polynomials fit to the whole data range. For N_2O, 1st-degree polynomial fit (red-dashed line) is only fit to data with mole fractions expected to be greater than 295 ppb. For SF_6, 1st-degree polynomial fit spans the entire data range.

Statement on data and archive availability for other studies and the amount of air stored in the tanks.

A statement on data availability is included at the end of the manuscript that we make all N_2O and SF_6 data available to the scientific community upon publication. The text in section 1 (page 4, line 13) states the current air pressure in archive canisters which ranges from 60-2000 kPa bar.

p. 1. l. 17.: is this precision for SF_6 not dependent on the mixing ratio, which has changed significantly during this time period?

The precision of measurement provided in the abstract and later in the section 2 (methods) is for current ambient mixing ratios and based on repeated analyses of the NOAA reference cylinder (328.71 ± 0.5 ppb N_2O, 8.76 ± 0.06 ppt SF_6). We have modified the language in the abstract to clarify this point as suggested. For archive samples, the absolute measurement precision was determined to be relatively consistent across the concentration range measured for N_2O and SF_6 based on replicate analysis (see error bars Fig. 5). However, relative precision of measurement for samples is dependent on the mixing ratio measured for SF_6 because of the wide range of mixing ratios in the archive. As noted, the result of this is the largest relative uncertainty is associated with the oldest samples where $SF_6 \leq 1$ ppt. Text in the main body now includes:

> *Mean measurement uncertainty (1σ) of OHSU-PSU air archive samples for N_2O is 0.23%. Mean measurement uncertainty (1σ) of SF_6 in the OHSU-PSU air archive samples ranges between 6.5% for samples below 1 ppt and 2.5% for samples at 4 ppt.*

P. 1. L. 29.: please specify that the stability is only valid for these compounds. Other gases may be much more critical.

We have updated the manuscript to include this change.

P. 2. L. 13.: also the temporal resolution of firn samples is limited.

We have updated the manuscript to include this change.

P. 2. L. 17.: I think it would be worthwile to add some comments here, especially mention the best known air archive, i.e. the one from Cape Grim, incl. some references to reanalysis from air archives, e.g. from Laube, Oram and Vollmer.

We agree with the reviewer and have updated the manuscript to include this change:

> *The most well-known air archive is that of Cape Grim, Tasmania (41° S, 145° E) in the southern hemisphere, containing samples dating back to 1978 (Vollmer et al. 2018).*

P. 2. L. 20.: a reference to the updated trend from the most recent WMO report (chapter1) could be made here).

We agree with the reviewer and have updated the manuscript to include this change:

> *The global mean mixing ratio of N_2O in 2017 was 329.8 ppb with a mean annual trend of 0.85 ppb yr^{-1} over the last 20 years (Dlugokencky et al. 2018).*

P. 3. L. 20.: please include some discussion on the recent re-evalution of the SF_6 atmospheric lifetime e.g. by Ray et al. 2017.

We have updated the manuscript to include this change.

P. 5. L. 22.: I think some discussion on the reproducibility for low SF_6 mixing ratios is necessary here. Does it differ from those of the NOAA standards? What is the implication for the reanalysis?

In terms of a study of the reproducibility at lower SF_6 mixing ratios, we were unable to perform a longer-term multi-day analyses as we did not have a sample of sufficient volume to do so (at low SF_6 mixing ratio). However, as the reproducibility tests at ambient SF_6 mixing ratios are very compatible with our analysis of the precision of measurement, we have no real reason to suspect the same study at lower mixing ratios would yield different results.

P. 6. l1ff.: Have the authors considered a cross interference between N_2O and CO_2? Are they separated chromatographically? If not then there could be a co-elution problem and then the dilution of the standard may result in a different matrix than in the case of air (which has shown different relative trends of CO_2 and N_2O). Co-elution of CO_2 and N_2O may effect the sensitivity of the detector, which impacts the non-linearity correction.

Our tests (using NDIR) indicate that CO_2 is well separated from N_2O on a 5.5m Porapak Q column.

P. 6. L. 23.: I think it is wrong to refer to measured N_2O here; this is the “linear-response” evaluation.

We have updated the manuscript to state “response evaluated” instead of “measured”.

P. 7. L. 3.: as above

We have updated the manuscript to state “response evaluated” instead of “measured”.

P. 7. L. 6.: a range of values for which such a linear correction has been applied should be given here also. Please use the newest AGAGE overall reference: Prinn et al., Earth System Sci. Data, 2018

We have updated the manuscript to include the range in values for which the linear corrections have been applied (with corrected values ranging between 298.9 – 314.8 ppb for N_2O and 0.6 – 4.3 ppt for SF_6).

P. 8. L. 25.: give years for the increase rates.

Years for the rate of increase the growth rates are calculated over are provided in the first sentence of the paragraph (1978 – 1996). However, we have added “over this same time period” to the end of the sentence to improve clarity.

P. 9. L. 13.: the ref. to Levin should be placed behind 1995.

We have updated the manuscript to include this change.

P. 9. L. 17.: as Edgar is largely derived from an inversion of observations, it is somewhat a circular argument to state that there is agreement.

In the case of SF_6, the reviewer makes a good point here that Edgar emissions inventories are based in-part of inversion of atmospheric measurements. However, atmospheric SF_6 data are particularly sparse in 1980s and early 1990s, particularly in the northern hemisphere where an overwhelming majority of emissions occur. Thus, the agreement between middle latitude northern hemisphere Cape Meares, OR (45N) data and EDGAR emissions inventory is useful for updating and improving emissions inventories.

P. 9. L. 31.: this sentence sounds funny.

We have restructured the sentence to the following:

> *Other mid-latitude northern hemisphere sites also show a seasonal phase similar to that observed at Cape Meares.*

P.10. L. 11.: is the seasonality independent of the mixing ratios? Otherwise please give the years for which this is valid.

So far as can be determined statistically, the seasonality observed at Cape Meares is independent of the mixing ratio.

P. 10. L. 24.: specify what you mean by vertical diffusion here.

We have updated the manuscript to not include vertical diffusion in the list of potential factors that may influence the observed seasonality at a location due to the ambiguity of the term.

p.11.l. 3: check grammar on this sentence.

We have updated the manuscript to the following:

> *The analysis of archived air samples gives the mole fraction of N_2O in 1980 to be 301.5 ± 0.3 ppb (1σ), rising to 313.5 ± 0.3 ppb (1σ) in 1996.*

Here we detail changes made in our revised manuscript in order to address particular points for the anonymous referee.

General and Specific Comments

Page 3, line 10. "Models have shown that future climate conditions will likely amplify N_2O production". Expand on this thought. Why is this so?

It is estimated that 44-73% of N_2O emissions originate from land ecosystems (Hirsch et al. 2006; Davidson et al. 2009). A warmer climate will most likely enhance these emissions (Arneth et al. 2010), driving a positive feedback loop. Stocker et al. (2013) investigates the role these feedback loops play in future climate conditions. We have updated the text to the following:

> *Models have shown that future climate conditions will likely amplify N_2O production through positive climate feedback effects, meaning a linear increase in time may under-predict future concentrations based on the current rate of change (Khalil and Rasmussen 1983; Stocker et al. 2013).*

Page 3, line 15. Add Hall et al. 2011

We have updated the manuscript to reflect this change.

Page 3, line 20. Consider adding the following citation for a recent estimate of SF_6 lifetime.

We have revised the manuscript to use updated estimates of the SF_6 lifetime from Kovacs et al. (2017) and Ray et al. (2017).

Page 5, line 4. How did you arrive at the detector temperature of 310 C? Was it optimized for N_2O and or SF_6?

The detector temperature of 310°C was used because we found that the response of the N_2O and SF_6 peaks were well defined at this temperature. Chromatogram output was optimized around N_2O while maintaining a robust SF_6 peak. No significant difference in detector response was found to using a detector temperature of 340°C reported in Hall et al. (2007) and Hall et al. (2011).

Page 5, line 9. Maybe not necessary to the paper. Why sample the archive air 6 times and then the reference gas 6 times instead of alternating between the two types of samples? Wouldn't alternating better track signal drift from injection to injection?

The procedure of running 6 measurements in a row of a sample or standard instead of alternating between standard and sample measurements was used because it was determined that while measuring N_2O, if a run contained an outlier (greater than 2σ), it was statistically more likely to be the first measurements (~30% of the time) compared to being in another position (~15% of the time). Outlier probability was evenly spread across measurement position for SF_6 (~17% for outlier to be in any position). The cause of this discrepancy for measurements of N_2O is unlikely to be contamination from a previous run as we are purging the sample loop (10 ml) with 9-times the sample loop volume (60 ml min^{-1} for 1.5 minutes). This memory effect is mitigated when running 6 measurements back to back. Drift in the detector response over a set of 6 measurements (~50 min) is assumed to be linear.

Page 7, Results. Can you comment on why there were some large outliers? Problems with the sample or the integrity of a few flasks? Were the outliers the same for both N_2O and SF_6? Why were two different criteria for residual outliers (2-sigma for N_2O and 3-sigma for SF_6) used?

Outliers in the OHSU-PSU air archive are possibly due to several factors including storage integrity or possible contamination during collection. It is unclear what exactly caused each of the far outliers evaluated.

For the initial filtering process, far outliers in the OHSU-PSU air archive were considered to be 6*MAD (median absolute deviation) for N_2O (removes 6 samples) and 7*MAD for SF_6 (removes 2 samples). The far outliers for N_2O are not the far outliers for SF_6. 7*MAD is used for SF_6 as opposed to 6*MAD because the annual increase in measured values for SF_6 (~10% yr^{-1}) is significantly larger than in N_2O (~0.25% yr^{-1}). It is important to note that roughly half of the 159 samples measured from the OHSU-PSU air archive date prior to 1985, meaning the median measured SF_6 mole fraction will be biased towards this early period. By using 7*MAD for SF_6, we only remove values that clearly lie outside of a reasonable measurement.

For the second filter, Polynomial fits (1st degree for N_2O and 2nd degree for SF_6) were applied to the data and residuals outside of 2σ for N_2O and 3σ for SF_6 were removed. 3σ was used for SF_6 because the data points fit tightly to the polynomial fit. The second filter removed another 6 samples for N_2O (for a total of 12) and another 2 samples for SF_6 (for a total of 4). Again, the outliers removed for N_2O are not the same samples removed for SF_6. We found that using 2σ for SF_6 removed data points unnecessarily from the analysis.

Page 7, line 20. It is uncertain to the reviewer what "bootstrapping residual variability 1000 times" means. Did you sample subsample the data 1000 times and re-smooth?

The bootstrap process consists of calculating a new value for each data point from a normal distribution with mean equal to the measurement and standard deviation equal to the residual variability found from the original LOWESS regression. We repeat the LOWESS regression calculation for the new data set. The process is completed 1000 times, from which we calculate the 95% confidence interval for the original LOWESS regression to the measured data.

Page 8, line 5. You could cite Geller et al. as well

We have updated the manuscript to reflect this change.

<u>Technical Corrections</u>

Page 1, line 14. "prior to" to "before"

We have updated the manuscript to reflect this change.

Page 2, line 22. "major" to "primary"

We have updated the manuscript to reflect this change.

Page 4, line 20. "Peak separation is achieved by two Poropak Q 80/100 mesh columns" to "Two Poropak Q 80/100 mesh columns achieve peak separation"

We have updated the manuscript to reflect this change.

Page 4, line 22. "to significantly improve baseline signal stability" to "to improve baseline signal stability significantly"

We have updated the manuscript to reflect this change.

Page 5, line 20. "a two-week period" to "two weeks"

We have updated the manuscript to reflect this change.

Page 6, line 4. "Error" to "The error"

We have updated the manuscript to reflect this change.

Page 6, line 6. "To characterize of the" to "To characterize the" (remove the "of")

We have updated the manuscript to reflect this change.

Page 6, line 8. "a N2O" to "an N2O"

The sentence has been reworded to:

> *To properly account for this interference,* SF_6 *dilutions at low mixing ratios (0.6 - 6.0 ppt) must have* N_2O *mole fractions that reflect expected mole fractions in archived samples (300 - 315 ppb).*

Page 7, line 17. “analysis” to “the analysis”

We have updated the manuscript to reflect this change.

Page 7, line 29. “Prinn et al.” is missing the period

We have updated the manuscript to reflect this change.

Page 9, line 12. Add a comma after Canada.

We have updated the manuscript to reflect this change.

Page 10, line 19. “have amplitude” to “have an amplitude”

We have updated the manuscript to reflect this change.

Page 10, line 22. “seasonal amplitude” to “the seasonal amplitude”

We have updated the manuscript to reflect this change.

Page 11, line 10. “and minimum amplitude” to “and a minimum amplitude”

We have updated the manuscript to reflect this change.

Trends in N_2O and SF_6 mole fraction in archived air samples from Cape Meares, Oregon (USA) 1978–1996

Terry C. Rolfe[1] and Andrew L. Rice[1]

[1]Department of Physics, Portland State University, Portland, 97201, United States

Correspondence to: Terry C. Rolfe (trolfe@pdx.edu)

Abstract. Quantifying historical trends in atmospheric greenhouse gases (GHG) is important to understanding changes in their budgets and for climate modeling which simulates historic and projects future climate. Archived samples analyzed using updated measurement techniques and calibration scales can reduce uncertainties in historic records of GHG mole fractions and their trends in time. Here, we present historical measurements of two important GHG, nitrous oxide (N_2O) and sulfur hexafluoride (SF_6), collected at the midlatitude northern hemisphere station Cape Meares, Oregon (USA, 45.5° N, 124° W) between 1978 and 1996 in archived air samples from the Oregon Health and Science University – Portland State University (OHSU–PSU) Air Archive. N_2O is the third most important anthropogenically forced GHG behind carbon dioxide (CO_2) and methane (CH_4). SF_6 has a low abundance in the atmosphere, but is one of the most powerful GHG known. Measurements of atmospheric N_2O made during this period are available for select locations but before~~prior to~~ mid-1990 have larger uncertainties than more recent periods due to advancements made in gas chromatography (GC) methods. Few atmospheric SF_6 measurements pre-1990 exist, particularly in the northern hemisphere. The GC system used to measure N_2O and SF_6 ~~concentration~~mixing ratios in this work is designed to be fully automated, capable of running up to 15 samples per batch. Measurement precision (1σ) of N_2O and SF_6 is 0.16% and 1.1% respectively (evaluated at 328.7 ppb and 8.8 ppt). Samples were corrected for detector response non-linearity when measured against our reference standard, determined to be 0.14 ppb ppb^{-1} in N_2O and 0.03 ppt ppt^{-1} in SF_6. The ~~concentration~~mixing ratio of N_2O in archived samples is found to be 301.5 ± 0.3 ppb in 1980 and rises to 313.5 ± 0.3 ppb in 1996. The average growth rate over this period is 0.78 ± 0.03 ppb yr^{-1} (95% CI). Seasonal amplitude is statistically robust, with a maximum anomaly of 0.3 ppb near April and a minimum near November of -0.4 ppb. Measurements of N_2O match well with previously reported values for Cape Meares and other comparable locations. The ~~concentration~~mixing ratio of SF_6 in analyzed samples is found to be 0.85 ± 0.03 ppt in 1980 and rises to 3.83 ± 0.03 ppt in 1996. The average growth rate over this period is 0.17 ± 0.01 ppt yr^{-1} (95% CI). Seasonality is statistically robust and has an annual peak amplitude of 0.04 ppt~~b~~ near January and a minimum amplitude of -0.03 ppt near July. These are unique SF_6 results from this site and represent a significant increase in SF_6 data available during the 1980s and early 1990s. The ~~concentration~~mixing ratio and growth rate of SF_6 measured compares well to other northern hemisphere measurements over this period. From these N_2O and SF_6 measurements, overall we conclude that sample integrity is robust in the OHSU-PSU Air Archive for N_2O and SF_6.

1 Introduction

Anthropogenic sources of greenhouse gases (GHG) have altered the atmospheric composition resulting in a significant climate forcing near 3 W m^{-2} since 1750 (Myhre et al. 2013). Measurements of GHG ~~concentration~~mixing ratios since the industrial revolution constrain global budget uncertainties and interpret recent changes to source and sink processes (Prinn et al. 2000; Khalil et al. 2002; Saikawa et al. 2014). When projecting future GHG ~~concentration~~mixing ratios, many additional factors must be included in models such as climate feedback effects and possible changes in transport processes. Uncertainties in model predictions can be minimized if GHG measurements are precise and span many different latitudes (Meinshausen et al. 2017).

When historical timeseries records are not available, past atmospheric GHG abundance can be evaluated using either archived air samples or by analysing ice core and firn air. One significant advantage of using ice core and firn air for measuring past atmospheric ~~concentration~~mixing ratios of GHG is that samples may be collected today that represent past conditions. However, ice core and firn samples are difficult to obtain due to the remoteness of the locations where the samples are collected (Greenland and Antarctica) and provide limited spatial information. Temporal uncertainties also must be evaluated when measuring ice core and firn samples due to diffusion and gravitational separation (Ishijima et al. 2007); samples are best represented by a mean age, limiting temporal resolution. By contrast, archived air samples are discrete in time and space, making them very valuable for evaluating past atmospheric abundance at specific periods in time. However, few air archives are available today. The most well-known air archive is that of Cape Grim, Tasmania (41° S, 145° E) in the southern hemisphere, containing samples dating back to 1978 (Vollmer et al. 2018). However, ~~A~~archive samples may ~~also~~ contain storage artefacts that can contaminate historical records and must be stored carefully to prevent damage or loss.

Nitrous oxide (N_2O) is the third most important GHG with anthropogenic sources after carbon dioxide (CO_2) and methane (CH_4). ~~Today, the concentration of N_2O is close to 330 ppb with a trend averaging 0.75 ppb yr^{-1} over the last 30 years (Ciais et al., 2013).~~ The global mean mixing ratio of N_2O in 2017 was 329.8 ppb with a mean annual trend of 0.85 ppb yr^{-1} over the last 20 years (Dlugokencky et al. 2018). N_2O has a large global warming potential (GWP), 298 times that of CO_2 over a 100-year period and a global radiative forcing estimated at 0.19 W m^{-2} since 1750 (Myhre et al., 2013). The long lifetime (~120 years) results in most emitted N_2O reaching the stratosphere, where photooxidation is the primary~~major~~ source of stratospheric NO_X ("active nitrogen"). NO_X is the main natural catalyst of ozone (O_3) destruction (Crutzen 1970).

Anthropogenic sources of N_2O account for roughly 40% of all N_2O emissions, with natural sources accounting for the other 60% (Ciais et al., 2013). Bottom-up calculations estimate anthropogenic production of 6.9 (2.7-11.1) TgN yr^{-1} and natural production of 11 (5.4-19.6) TgN yr^{-1}. The uncertainty in these estimations is large, with 1σ error nearly ± 50%. Together with atmospheric measurements, top-down modelling better constrains the N_2O budget and reduces uncertainty in the global source. Sources of N_2O calculated this way estimate anthropogenic and natural source production of 6.5 (5.2-7.8) TgN yr^{-1} and 9.1 (8.1-10.1) TgN yr^{-1}, respectively (Prather et al., 2012).

There are three major natural sources and six major anthropogenic sources of N_2O. Natural sources of N_2O are natural soils (3.3-9.0 TgN yr^{-1}), oceans (1.8-9.4 TgN yr^{-1}), and atmospheric chemistry (0.3-1.2 TgN yr^{-1}) (Note: sources include the minimum and maximum estimates provided from bottom-up calculations in Ciais et al., 2013). By far, the largest anthropogenic source is agriculture, producing 1.7-4.8 TgN yr^{-1}, followed by industrial and fossil fuel sources (0.2-1.8 TgN yr^{-1}), biomass burning (0.2-1 TgN yr^{-1}), rivers and estuaries (0.1-2.9 TgN yr^{-1}), atmospheric deposition (0.4-1.3 TgN yr^{-1}), and human excreta (0.1-0.3 TgN yr^{-1}) (Ciais et al. 2013). More constraints on source production provided through atmospheric measurements are needed to improve estimates of individual source magnitudes.

The main loss mechanism for N_2O is destruction in the stratosphere through photolysis and the reaction with $O(^1D)$ (Prather et al. 2015). Soils and the oceans can act as sinks for N_2O through microbial processes, however because the production of N_2O is greater than what is consumed, the global net flux is positive. Estimates of the stratospheric sink account for 11.9 (11.0-12.8) TgN yr^{-1} (Ciais et al., 2013).

Rising global ~~concentration~~mixing ratios of N_2O are due to the imbalance between the sources and the sinks. Based on a top-down constraint, the imbalance between sources and sinks is 3.6 (3.5-3.8) TgN yr^{-1} (Ciais et al., 2013).

Models have shown that future climate conditions will likely amplify N_2O production through positive climate feedback effects, meaning a linear increase in time may under-predict future ~~concentration~~mixing ratios based on the current rate of change (Khalil and Rasmussen 1983; Stocker et al. 2013). To minimize uncertainty in the N_2O budget and in model projections, precise measurements of current and past atmospheric conditions from multiple global locations are needed. Measurements of atmospheric N_2O made prior to mid-1990 have larger uncertainties than more recent periods due to advancements made in gas chromatography (GC) methods (Prinn et al. 2000; Jiang et al. 2007; Hall et al. 2011). To reduce uncertainty during this period, archived samples may be analyzed using updated measurement techniques. Additionally, measurements of the isotopic composition of N_2O in archived samples can constrain the N_2O budget and changes in time due to characteristic isotopic effects in sources and sinks (Park et al. 2012; Snider et al. 2015).

Sulfur hexafluoride (SF_6) is an extremely potent GHG. Recent estimates calculated the GWP to be 22800 (over 100 years compared to CO2) and an atmospheric lifetime of 580-1475 years (Kovács et al. 2017; Ray et al. 2017). ~~with a GWP of 22800 (over 100 years compared to CO_2) and a lifetime of ∼3200 years (Ravishankara et al. 1993).~~ While SF_6 is one of the strongest GHG controlled under emission regulations, it has a low global ~~concentration~~mixing ratio (9.3 ppt in the northern hemisphere in 2017~~7.29 ppt in 2011~~), so it does not add significantly to climate forcing by itself (Prinn et al. 2018~~Myhre et. al. 2013~~).

Sources of SF_6 are anthropogenic, with main uses being high voltage insulation, magnesium production and semiconductor manufacture (Maiss and Brenninkmeijer 1998; Olivier et al. 2005). Global production in 2008 was estimated to be 7.16 Gg yr^{-1} (Levin et al. 2010). With a very low solubility and no reactivity in the lower atmosphere, the only known sink for SF_6 is loss in the mesosphere.

With almost all of the SF_6 that has been emitted since the industrial revolution to the atmosphere still present, global emissions can be accurately determined from observations of atmospheric ~~concentration~~mixing ratio. Due to its long lifetime and anthropogenic origins, SF_6 is used as a validity check for atmospheric transport models (Levin and Hesshaimer, 1996; Patra et al., 2009). It has been estimated that 94% of all SF_6 emissions originate in the northern hemisphere (Maiss et al. 1996), explaining a north-south hemisphere gradient in SF_6 ~~concentration~~mixing ratio of about 0.4 ppt (Levin et al. 2010).

Observations of the growth rate have been reported by several studies (Levin et al. 2010; Rigby et al. 2010; Hall et al. 2011). The trend in SF_6 has varied over the last 30+ years and while the magnitude of the growth rate differs slightly between sample locations, several features are prominent. From the early 1970s to the mid-1990s, the trend steadily increased from 0.1 ppt yr^{-1} and peaked near 0.26 ppt yr^{-1}. The trend then slowly declined to ~0.20 ppt yr^{-1} until the early 2000s, when the trend increased again. The inferred global emission of SF_6 from the trend increases nearly linearly from 2 Gg yr^{-1} in the late 1970s to over 6 Gg yr^{-1} in 1994-1995 (Levin et al. 2010; Rigby et al. 2010).

Reported atmospheric measurements of SF_6 before the year 1987 are few. In the southern hemisphere, Cape Grim, Tasmania (41° S, 145° E) archive measurements date back to 1978 (Levin et al. 2010). Northern hemisphere measurements are reported dating from 1973 from Trinidad Head, CA (41° N, 121° W), but few are prior to 1990 (Rigby et al. 2010). A more complete record of past SF_6 atmospheric ~~concentration~~mixing ratios is desirable.

The Oregon Health & Science University–Portland State University (OHSU-PSU) air archive includes archived air samples collected from Cape Meares, Oregon (45.5° N, 124.0° W) in the late 1970s, 1980s, and 1990s by the Department of Environmental and Bimolecular Systems, Oregon Graduate Institute of Science and Engineering (currently OHSU). The samples were collected by air liquefaction, where ~1000 L (STP) of dried air ~~(STP)~~(using a condenser) was compressed to 3000 kPa into 33 L electropolished stainless steel canisters. Today, archive samples are stored at Portland State University and contain pressures ranging from 60-2000 kPa (Rice et al. 2016). Here, we present details of the analytical technique employed and results from the analysis of 159 Cape Meares air samples from the OHSU-PSU air archive.

2 Methods

2.1 Gas chromatography analytical system

The gas chromatography (GC) analytical system (Fig. 1) employed at Portland State University for measuring N_2O and SF_6 in archived air samples is based on the configuration used by Hall et al. (2007) and references therein. We use an Agilent model 6890N gas chromatograph fitted with a micro-electron capture detector (µECD, Agilent Technologies, Santa Clara, CA). ~~Peak separation is achieved by t~~Two Poropak Q 80/100 mesh columns (1.8 m × 2 mm i.d. pre-column, 3.7 m × 2 mm i.d. analytical column) achieve peak separation. The carrier gas is P5 (99.999%, Airgas, Portland, OR) equipped with O_2 and hydrocarbon traps (Restek, Bellefonte, PA) to further reduce impurities and found to ~~significantly~~ improve baseline signal stability significantly. Two six-port switching valves (V_1 and V_2), a four-port switching valve (V_3), and a 16-port multi-position valve (Valvo Instrument Company Inc., Houston, TX) are controlled through Chemstation (V1.A, Agilent Technologies Inc., Santa Clara, CA).

A sample run begins in “back-flush” mode, with carrier gas flushing the pre-column in the reverse analytical direction to remove the build-up of water on the analytical column that would otherwise eventually elute to the µECD and affect signal baseline. A 16-port multi-position valve is used to introduce pressurized samples into the system; a 2-way electric valve (Clippard, Cincinnati, OH) is used to stop sample flow to the sample loop and prevent sample loss. Samples initially pass through a desiccant trap (Perma Pure, Toms River, NJ), before flushing a 10 ml sample loop at 60 ml min^{-1} for 1.5 minutes. At this time, V_3 rotates, which places the system in “front-cut” mode and allows the sample loop to equilibrate. V_1 rotates at 1.75 minutes and allows the carrier gas to carry the sample N_2O and SF_6 to the pre-column where separation from O_2 and H_2O occurs. After O_2 elutes through the pre-column to vent, at 3 minutes V_2 rotates and places the pre-column in line with the analytical column, transferring N_2O and SF_6 to the analytical column. At 4.25 minutes, the sample has reached the analytical column and V_1, V_2, and V_3 rotate. This begins the back-flush of the pre-column while the analytes are carried to the µECD on the analytical column.

Oven and detector temperatures are maintained at 56° C and 310° C respectively. Carrier gas flow rates are 40 ml min^{-1} maintained by electronic pressure control of the 6890N. N_2O peak retention time is 6.1 minutes and SF_6 peak retention time is 7.0 minutes (Fig. 2). Peak integration is accomplished via Chemstation based on peak height.

All measurements of N_2O and SF_6 are made relative to a calibrated whole air sample on the NOAA-06A N_2O scale and NOAA-14 SF_6 scale (NOAA Tank CB11406-A, 328.71 ± 0.5 ppb N_2O, 8.76 ± 0.06 ppt SF_6), here-on referred to as the NOAA reference gas. Each sample is analysed 6 times and bracketed by 6 reference gas runs used to measure instrument response and track signal drift. The GC-µECD analytical system was evaluated for precision, reproducibility, and linearity prior to its application to measure mole fraction in historic archive samples.

2.2 Precision and reproducibility of analytical system

Precision of measurement was determined by repeated analysis of the reference standard~~comparing residuals from sets of 6 gas analyses~~. Histogram distributions in figure 3 show 180 residuals (expressed as a percent relative standard deviation) collected from 30 sets of 6 measurements of N_2O (Fig. 3a) and SF_6 (Fig. 3b) of the NOAA reference gas. Both N_2O and SF_6 compare well to a normal distribution (black dashed lines), with chi-square goodness of fit p-values of 0.16 and 0.35, respectively. For N_2O, $1\sigma = 0.16\%$ while for SF_6, $1\sigma = 1.1\%$. This corresponds to an uncertainty of ± 0.52 ppb for N_2O and ± 0.10 ppt for SF_6. Mean measurement uncertainty (1σ) of OHSU-PSU air archive samples for N_2O is 0.23%. Mean measurement uncertainty (1σ) of SF_6 in the OHSU-PSU air archive samples ranges between 6.5% for samples below 1 ppt and 2.5% for samples at 4 ppt.

Measurement reproducibility was evaluated by repeatedly measuring a dry air sample (Breathing Air, Airgas, Portland, OR) against the NOAA reference gas and evaluating consistency from the standard deviation of the results. The sample was measured 18 times over~~ a~~ two weeks~~-week period~~ with mean measured ~~concentration~~mixing ratios of N_2O and

SF_6 of 390.9 ppb and 13.2 ppt, respectively. The standard deviations in N_2O and SF_6 measurements are 0.46 ppb and 0.11 ppt respectively, which are indistinguishable from 1σ precision for a set of 6 NOAA reference gas measurements.

2.3 Linearity of the GC- μECD system

To ensure accurate results for this work, the detector response was evaluated over the mole fraction range expected for N_2O and SF_6 in the OHSU-PSU Air Archive. The range in northern hemisphere N_2O mole fraction between 1978 and 1996 is between 295 and 314 ppb (Prinn et al. 2000; Ciais et al. 2013). Archived air sample measurements of northern hemisphere SF_6 mole fraction from Trinidad Head, CA measure below 1 ppt in the 1970s and rise to nearly 4 ppt in 1997; southern hemisphere measurements from Cape Grim, Tasmania and the South Pole show a similar range (Levin et al. 2010; Rigby et al. 2010).

A series of manometric dilutions were prepared from the NOAA reference gas at Portland State University to evaluate the μECD response over historical N_2O and SF_6 mole fraction sample range. To characterize the N_2O response, the N_2O reference gas was diluting with ultra-pure air (zero grade, Airgas, Portland, OR; N_2O and SF_6 at ~~concentration~~mixing ratios below detection limits) using capacitance manometers (MKS Instruments, Andover, MA; range 0-10 torr and 0-1000 torr) into 3L electropolished stainless steel canisters (precision ± 0.01%). The range of N_2O ~~concentration~~mixing ratios produced in 3 L canisters was 32.2 - 321.4 ppb. The ~~E~~error introduced from the manometric process is small when compared to measurement uncertainty (maximum 1σ error of ± 0.07 ppb for N_2O).

To characterize~~ of~~ the SF_6 response at low ppt ~~concentration~~mixing ratios requires consideration of the effect of the falling N_2O tail on the chromatogram baseline. To properly account for this interference, SF_6 dilutions at low ~~concentration~~mixing ratios (0.6 - 6.0 ppt) must have~~ a~~ N_2O ~~concentration~~mole fractions that reflect~~s~~ expected ~~concentration~~mixing ratios in archived samples (300~~2~~–3154 ppb). Prepared dilutions of SF_6 included the addition of an aliquot of 1 ppm N_2O (±5%, Scott Specialty Gases, St. Louis, MO) into the canister prior to dilution with ultra-pure air. The maximum error (1σ) in SF_6 introduced from the manometric process is small (0.001 ppt) compared to measurement uncertainty. However, SF_6 present in either ultra-pure air dilution gas or the N_2O aliquot at trace levels below the detection limit of our measurement (<0.1 ppt) contribute to the uncertainty in prepared samples. All dilution samples were measured at PSU on the GC-μECD system over several weeks to account for instrument drift. Tables 1 and 2 provide~~s~~ dilution sample pressures, calculated and observed μECD response, and measured N_2O and SF_6 mole fractions with the error in measurement used to characterize the GC-μECD linearity.

Results of linearity experiments are shown in figure 4. For N_2O, a slope of 0.8747~~0~~ ± 0.028 (95% CI) is found over the data range 289.7 - 328.7 ppb, most relevant for this work. A linear fit is a good model for the deviation from expected over this range ($R^2 = 0.964$); additional polynomial terms are not statistically robust. This results in sample measurements deviating from expected by ~0.14 ppb ppb^{-1} N_2O difference from the NOAA reference. For the range of the N_2O in the OHSU-PSU air archive, all N_2O samples are adjusted for a linear correction of the form:

$[N_2O]_X = a_1[N_2O]_Y + a_2$ (1)

a_1 = 1.143~~6~~ ± 0.037 *(95% CI)* (2)

a_2 = -47.24~~95~~ ± 11.49 *(95% CI)* (3)

Where $[N_2O]_Y$ is the response evaluated~~measured~~ N_2O mole fraction and $[N_2O]_X$ is the corrected value. The slope and y-intercept, as well as their 95% confidence intervals, are represented by a_1 and a_2 respectively. This correction is applied to all sample N_2O measurements (corrected values ranging between 298.9 – 314.8 ppb).

The entire NOAA reference gas dilution range for N_2O (32 - 321 ppb) results in a deviation that can be adequately modeled using a 3rd degree polynomial. The linear fit discussed above is indistinguishable from the full 3rd degree polynomial over the N_2O ~~concentration~~mixing ratio range of the OHSU-PSU Air Archive. However, if measuring N_2O samples with a difference of more than 80 ppb compared to the NOAA reference gas, the full 3rd degree polynomial is necessary to correct for the non-linear response in the µECD.

For SF_6, the prepared sample range over which the linear correction is applied is 0.59 – 8.76 ppt, most relevant for this work. The slope of the SF_6 linear fit is 0.9728~~1~~ ± 0.017 (95% CI) and is a good model for the deviation from expected over this range (R^2 = 0.9995). This results in a deviation from expected of ~0.03 ppt ppt^{-1} SF_6 difference from the NOAA reference when measuring samples. All SF_6 measurements are adjusted for a linear correction of the form:

$[SF_6]_X = b_1[SF_6]_Y + b_2$ (4)

b_1 = 1.028~~3~~ ± 0.018 *(95% CI)* (5)

b_2 = -0.294~~7~~ ± 0.099 *(95% CI)* (6)

Where $[SF_6]_Y$ is the response evaluated~~measured~~ SF_6 mole fraction and $[SF_6]_X$ is the corrected value. The slope and y-intercept, as well as their 95% confidence intervals, are represented by b_1 and b_2, respectively. This correction is applied to all sample SF_6 measurements (corrected values ranging between 0.6 – 4.3 ppt).

Detector response non-linearity has been evaluated in previous work by other groups on GC-ECD systems. For N_2O, deviations from expected of ~ 0.2 ppb ppb^{-1} difference from the reference gas are reported when in the linear range are typical (Schmidt et al. 2001; Hall et al. 2007). These are similar to the value reported here for the µECD. Over larger ranges, a similar non-linear response curve is also reported. SF_6 non-linearity reported in Levin et al. (2010) has a similar curvature to the full N_2O non-linear response previously discussed. Yet, this curvature is not observed to be significant over the range of SF_6 dilutions conducted here.

3 Results and Discussion

3.1 Air archive mole fractions of N_2O and SF_6

Measurements of N_2O and SF_6 mole fraction from 159 samples of the OHSU-PSU Air Archive were initially filtered for analysis using a 7 median absolute deviation (7MAD) noise filter to remove far outliers. Polynomial fits (1st degree for N_2O and 2nd degree for SF_6) were then applied to the data. Residual values outside of 2σ for N_2O and 3σ for SF_6

were removed for further data analysis. The entire process removed 12 data points for N_2O and 4 data points for SF_6 used in the analysis.

Deseasonalized measurements of N_2O and SF_6 from Cape Meares are shown in figure 5a and 5b, respectively. A locally weighted linear regression (LOWESS) is used to smooth the data using a 3-year smoothing window (Cleaveland and Devlin 1988). The confidence intervals around regressions are calculated by bootstrapping residual variability 1000 times. The regression results in a N_2O mole fraction ~~concentration~~ of 301.5 ± 0.3 ppb (1σ) in 1980 and increasing roughly linearly to the mid 1990s, where the ~~concentration~~mixing ratio is 313.5 ± 0.3 ppb (1σ) in 1996.

Observations of N_2O mole fraction match well with previously published measurements of N_2O from Cape Meares between 1978 and 1998 of 301.2 ppb in 1980 and 313 - 314.5 ppb in 1996 on the SIO-1998 N_2O scale (Prinn et al. 1990; Prinn et al. 2000; Khalil et al. 2002). The N_2O scale difference between SIO-1998 and NOAA-06 is minimal (Hall et al. 2007). Additional measurements by the Advanced Global Atmospheric Gases Experiment (AGAGE) and NOAA/ESRL (on the SIO-1998 N_2O and NOAA-06 N_2O scales, respectively) are reported from comparable sample locations. Trinidad Head, CA (41° N, 121° W), Mace Head, Ireland (53° N, 10° W), and Niwot Ridge, CO (40° N, 106° W) all measure ~313 ppb in 1996 (Prinn et al. 2000; Hall et al. 2007). Together, these comparisons indicate the N_2O in the archived samples has stored well.

Measured SF_6 ~~concentration~~mixing ratio in archived Cape Meares samples is determined to be 0.85 ± 0.03 ppt (1σ) in 1980 and increases to a ~~concentration~~mixing ratio of 3.83 ± 0.03 ppt (1σ) in 1996. Cape Meares does not have previously reported measurements of SF_6 to compare with directly. Measurements of SF_6 from Trinidad Head, CA are reported to be ~0.85 ppt in 1980 and ~3.73 ppt in 1996 on the SIO-2005 SF_6 scale (Rigby et al. 2010). To convert to the NOAA-06 SF_6 scale, values measured on the SIO-2005 SF_6 scale are divided by a conversion factor of 0.9991 (Hall et al. 2014). In 1996, values of 3.87 ppt, 3.87 ppt, and 3.78 ppt are reported for Alert, Canada (82° N, 62° W), Barrow, AK (71° N, 157° W), and Niwot Ridge, CO respectively on the NOAA-06 SF_6 scale (Hall et al. 2011). At these SF_6 ~~concentration~~mixing ratios, the difference between the NOAA-06 scale and the NOAA-14 scale is minimal. Cape Meares SF_6 measured values compare well with these northern hemisphere locations.

In the northern hemisphere, maximum background ~~concentration~~mixing ratio measurements of SF_6 are reported from mid-to-high latitudes (Geller et al. 1997). For the year 1994, measurements from Fraserdale, Canada (50° N, 82° W) are reported to be 0.14 ppt higher than samples measured from Izaña, Tenerife (28° N, 16° W) (Maiss et al. 1996). This difference is explained by the vast majority of SF_6 emissions coming from the mid-latitudes in the northern hemisphere (Maiss and Brenninkmeijer 1998; Levin et al. 2010; Rigby et al. 2010). The measured SF_6 ~~concentration~~mixing ratios from Cape Meares, also a midlatitude NH site, appear to fit in well with the expected meridional gradient when comparing to previously mentioned reported values.

Southern hemisphere measurements of SF_6 from archived atmospheric samples from Cape Grim, Tasmania (41° S, 145° E) and Neumayer, Antarctica (70° S, 8° W) are ~0.6 – 0.7 ppt in 1980 and ~3.4 – 3.5 ppt in 1996 on SIO-2005 and University of Heidelberg SF_6 scales (Levin et al. 2010, Rigby et al. 2010). As with the SIO-2005 SF_6 scale, the NOAA-06 and University of Heidelberg scale differences are small. To convert to the NOAA-06 SF_6 scale, values measured on the University of Heidelberg SF_6 scale are divided by a conversion factor of 0.9954 (Hall et al. 2014). Including a scale correction, Cape Meares SF_6 measurements are higher than Cape Grim and Neumayer during this period by 0.2 - 0.4 ppt. Much or all of this difference can be explained by an interhemispheric north-south difference of 0.3 – 0.4 ppt (Levin et al. 2010).

3.2 Growth rate in N_2O and SF_6

The mean secular trend between 1978 and 1996 for N_2O and SF_6 is 0.78 ± 0.03 ppb yr^{-1} (95% CI) and 0.17 ± 0.01 ppt yr^{-1} (95% CI) respectively, determined by applying a linear fit to deseasonalized data over this time period. These trends translate to annual increases of ~ 0.25% and ~ 0.1% for N_2O and SF_6, respectively. Annual trends for N_2O and SF_6 at Cape Meares, Oregon are determined from the derivative of the deseasonalized localized regression (Fig. 5 c&d). Uncertainty bands are generated from regressions of bootstrapped variability. Data points represent the mean annual trend with error bars equal to ±1σ of the trend over the year.

The mean annual trend in N_2O (Fig. 5c) ranges between 0.6 ppb yr^{-1} and 1.2 ppb yr^{-1}. All years between 1980 and 1996 show a positive rate of change significant at the 95% confidence level. The uncertainty in the annual trend is smallest in the early 1980s, at ± 0.15 ppb yr^{-1} (95% CI), where there are largest numbers of data (~50% of samples are between 1980 and 1985). After 1985, uncertainty in the annual trend becomes ± 0.5 ppb yr^{-1} (95% CI). This relatively large uncertainty results in an annual growth rate that is statistically indistinguishable between years.

A previously reported secular trend of N_2O reported between 1978 and 1998 for Cape Meares is 0.74 ± 0.02 ppb yr^{-1} indistinguishable from our result (Prinn et al. 2000). The global secular trend of N_2O for the period 1985 to 1996 reported by Khalil et al. (2002) is 0.69 ± 0.03 ppb yr^{-1}, also compatible with our trend at Cape Meares.

The SF_6 annual trend (Fig. 5d) from the Cape Meares analysis increases from 0.07 ± 0.03 ppt yr^{-1} (95% CI) in 1980 to 0.26 ± 0.05 ppt yr^{-1} (95% CI) in 1994. The average rate of change in the growth rate (second derivative of mole fraction vs. time) over this period is 0.014 ppt yr^{-2}. The increase in growth rate over this period is statistically significant at high levels of confidence (95%). After 1994, we measure a decrease in the growth rate, though this decline is not statistically significant at high levels of confidence over this short time interval.

Comparable trends in SF_6 measured at other locations are available for the mid-1990s. The average global growth rate of SF_6 in 1994 was reported at 0.23 ppt yr^{-1} in the northern hemisphere (Maiss et al. 1996). Alert, Canada, and Izaña, Tenerife are observed to have maximum trends of 0.26 ppt yr^{-1} in mid-1994 and at the beginning of 1995 (Levin et al. 2010), respectively, compatible with results presented here ~~(Levin et al. 2010)~~. This localized maximum in growth rate is present in some southern hemisphere observations of SF_6 at a similar time as well; Neumayer, Antarctica shows a maximum trend in 1995-1996 of 0.25 ppt yr^{-1} (Levin et al. 2010). This finding is consistent with a peak in SF_6 emissions as reported by the European Database for Global Atmospheric Research (EDGAR, v4.2).

Another feature observed in the SF_6 trend from Cape Meares is a local maximum in the growth rate near 1987 (Fig. 5d). Notably however, not all data sets agree. The growth rate reported from Neumayer, Antarctica has this feature during a similar period (Levin et al. 2010), but the trend reported at Cape Grim, Tasmania does not show this local maximum (Rigby et al. 2010). Due to the large uncertainty from the few archived samples available during that time period, this local maximum is not statistically distinguishable from surrounding years at high levels of confidence in the Cape Meares analysis and this result is merely suggestive. Additional evidence is needed to corroborate this finding.

3.3 Seasonality in N_2O and SF_6 mole fraction

Seasonal behaviour for N_2O and SF_6 are shown in figure 6 determined from residuals to the secular trend. The N_2O seasonal cycle at Cape Meares shows a maximum near April and May of 0.3 ppb and an extended minimum from September through December of –0.4 ppb. Although there is considerable uncertainty surrounding monthly means, the difference between the spring maximum and fall minimum is statistically robust at high levels of confidence (2-sample KS test p-value = 0.003).

The seasonal amplitude matches well with previously reported northern hemisphere magnitudes of ± 0.4 ppb (Liao et al. 2004). Other mid-latitude northern hemisphere sites also show a seasonal phase similar to that observed at Cape Meares.~~Seasonal phase is also similar to Cape Meares at other mid-latitude northern hemisphere sites.~~ N_2O seasonality reported at Mace Head, Ireland has a maximum near April and a minimum near August and September (Nevison et al. 2004; Jiang et al. 2007) and Trinidad Head, CA seasonality has a maximum near late May and a broad minimum from September to January (Nevison et al. 2007).

In general, N_2O seasonal amplitude is known to vary strongly with latitude, e.g., 0.29 ppb at the South Pole (90° S, 102° W) and 1.15 ppb at Alert, Canada (Jiang et al. 2007). This is attributed in part to the stronger branch of the Brewer Dobson circulation in the northern hemisphere which also explains the high latitude minimums in late-summer months related to the influx of N_2O depleted air from the stratosphere during the spring (Liao et al. 2004; Nevison et al. 2004). Aside from atmospheric circulation, N_2O seasonality may also be influenced by regional sources. L~~e~~ueker et al. (2003) suggested local maximums at Trinidad Head may reflect the influence of strong coastal upwelling. Similarly located in the Eastern Pacific, Cape Meares may also be subject to coastal upwelling influences. Isotopic analysis or modeling of transport effects and source influence would be useful to help interpret seasonal behaviour of N_2O at Cape Meares.

Seasonality for SF_6 shows a maximum between December and February of 0.04 ppt and a minimum near July of -0.03 ppt. The difference between the winter maximum and summer minimum is statistically significant (2-sample KS test p-value = 0.004). SF_6 seasonality has not previously been reported for Cape Meares.

Some seasonality in northern hemisphere observations of SF_6 is reported in the literature at select locations. Barrow, AK has a minimum in September and October with a broad maximum from December to June (Patra et al. 2009). Alert, Canada shows a strong minimum in October, though a maximum is not clearly defined (Wilson et al. 2014). Continental sites such as Niwot Ridge show large interannual variability (IAV) but have little distinguishable seasonality (Patra et al. 2009).

SF_6 seasonality at Cape Grim has been reported to have an amplitude of ± 0.01 ppt with a maximum in September and October and a minimum in near February (Nevison et al. 2007; Wilson et al. 2014). The seasonality phase of Cape Grim is nearly anti-phase of Cape Meares reported here, though the amplitude is a factor of 4 smaller at Cape Grim. Similar to N_2O, the seasonal amplitude is expected to be larger in the northern hemisphere than in the southern hemisphere (Nevison et al. 2007). Because sources of SF_6 are a-seasonal and sinks are essentially zero in the troposphere, the driving force behind the observed seasonality in SF_6 is considered to be atmospheric transport (Patra et al. 2009). Processes such as convection, ~~vertical diffusion,~~ boundary layer mixing, stratosphere-troposphere exchange (STE), and shifts in the ITCZ can potentially influence the observed seasonality at a location. Seasonal transport from STE adds relatively depleted SF_6 air into the troposphere from the stratosphere. The seasonal phase of SF_6 observed at Cape Meares closely reflects seasonality phasing observed in CFCs in the northern hemisphere driven by STE (Liang et al. 2008). Modeling atmospheric transport effects on SF_6 at Cape Meares could help confirm amplitude and phase reported here.

4 Conclusions

We have measured 159 samples from the OHSU-PSU Air Archive from Cape Meares, Oregon (45.5° N, 124.0° W) for N_2O and SF_6 mole fraction using GC-µECD spanning April 1978 to December 1996. The GC-µECD system is designed to be fully automated, capable of running multiple pressurized samples per run. Measurement precision of N_2O and SF_6 is 0.16% and 1.1% respectively. Sample ~~concentration~~mixing ratios were also corrected for detector response non-linearity when measured against our reference gas. The linearity correction was found to be 0.14 ppb ppb^{-1} and 0.03 ppt ppt^{-1} for N_2O and SF_6, respectively.

The ~~A~~analysis of archived air samples gives~~finds~~ the mole fraction of N_2O in 1980 to be 301.5 ± 0.3 ppb (1σ), ~~and~~ rising~~es~~ to 313.5 ± 0.3 ppb (1σ) in 1996. The average growth rate over this period is 0.78 ± 0.03 ppb yr^{-1} (95% CI). Seasonality shows peak amplitude of 0.3 ppb near April and minimum amplitude of -0.4 ppb near November and is statistically robust. Our measurements of N_2O were found to match well with previously reported values for Cape Meares and other comparable northern hemisphere mid-latitude locations.

For SF_6, the ~~concentration~~mixing ratio in 1980 is found to be 0.85 ± 0.03 ppt (1σ), increasing to 3.83 ± 0.03 ppt (1σ) in 1996. The average growth rate over this period is 0.17 ± 0.01 ppt yr^{-1} (95% CI). Seasonality shows peak amplitude of 0.04 ppb near January and a minimum amplitude of -0.03 ppt near July. There are no previous reported measurements of SF_6 from Cape Meares to compare against directly. SF_6 measurements compare well to other northern hemisphere measurements from Levin et al. (2010), Rigby et al. (2010), and Hall et al. (2011) over similar time periods when including spatial variability. From these N_2O and SF_6 measurements, we can conclude the sample integrity is robust within the OHSU-PSU

Air Archive from Cape Meares, Oregon. Resulting dataset of SF_6, in particular, contributes to a better characterization of historic SF_6 growth rate and its atmospheric variability over this period of dramatic growth.

Competing interests

The authors declare that they have no conflict of interest.

Acknowledgements

This study was supported by the US National Science Foundation (Atmospheric and Geospace Sciences grant 0952307). The authors would like to recognize Johnathan Radda for his assistance developing the GC-µECD technique used to measure the samples, R. A. Rasmussen for help establishing the OHSU-PSU air archive, and Christopher Butenhoff and M. A. K. Khalil for their assistance with data analysis and interpretation.

Data availability: A supplementary dataset of N_2O and SF_6 mole fractions at Cape Meares, Oregon measured for this work from the OSHU-PSU Air Archive are available to the scientific community (upon publication) and may be obtained by contacting the corresponding author.

References

Ciais, P., Sabine, C., Bala, G., Bopp, L., Brovkin, V., Canadell, J., Chhabra, A., DeFries, R., Galloway, J., Heimann, M., Jones, C., Le Quéré, C., Myneni, R.B., Piao, S., and Thornton, P.: Carbon and Other Biogeochemical Cycles. In: Climate Change 2013: The Physical Science Basis. Contribution of Working Group I to the Fifth Assessment Report of the Intergovernmental Panel on Climate Change [Stocker, T.F., Qin, D., Plattner, G.-K., Tignor, M., Allen, S.K., Boschung, J., Nauels, A., Xia, Y., Bex, V., and Midgley, P.M. (eds.)]. Cambridge University Press, Cambridge, United Kingdom and New York, NY, USA, 2013.

Crutzen, P.: The influence of nitrogen oxides on the atmospheric ozone content, Quarterly Journal of the Royal Meteorological Society, 96(408), 320-325, 1970.

Cleveland, W. S., and Devlin, S. J.: Locally weighted regression: An approach to regression analysis by local fitting, Journal of the American Statistical Association, 83(403), 596-610, 1988.

Dlugokencky, E. J., Hall, B. D., Montzka, S. A., Dutton, G., Mühle, J., and Elkins, J. W.: Atmospheric composition: Long-lived Greenhouse Gases [in "State of the Climate in 2017"]. Bull. Amer. Meteor. Soc., 99 (8), S46–S49, doi:10.1175/2018BAMSStateoftheClimate.1, 2018.

EDGAR, Emission Database for Global Atmospheric Research (EDGAR): European Commission, Joint Research Centre (JRC)/Netherlands Environmental Assessment Agency (PBL), release version 4.2., http://edgar.jrc.ec.europa.eu, 2013.

Geller, L., Elkins, J., Lobert, J., Clarke, A., Hurst, D., Butler, J., and Myers, R.: Tropospheric SF6: Observed latitudinal distribution and trends, derived emissions and interhemispheric exchange time. Geophys. Res. Lett.,24(6), 675-678, 1997.

Hall, B. D., Dutton, G. S., and Elkins, J. W.: The NOAA nitrous oxide standard scale for atmospheric observations. J. Geophys. Res.-Atmos., 112, D09305, doi:10.1029/2006JD007954, 2007.

Hall, B. D., Dutton, G. S., Mondeel, D. J., Nance, J. D., Rigby, M., Butler, J. H., Moore, F. L., Hurst, D. F., and Elkins, J. W.: Improving measurements of SF6 for the study of atmospheric transport and emissions, Atmos. Meas. Tech., 4(11), 2441-2451, 2011.

Hall, B. D., Engel, A., Mühle, J., Elkins, J. W., Artuso, F., Atlas, E., Aydin, M., Blake, D., Brunke, E.-G., Chiavarini, S., Fraser P. J., Happell, J., Krummel, P. B., Levin, I., Loewenstein, M., Maione, M., Montzka, S. A., O'Doherty, S., Reimann, S., Rhoderick, G., Saltzman, E. S., Scheel, H. E., Steele, L. P., Vollmer, M. K., Weiss, R. F., Worthy, D., and Yokouchi, Y.: Results from the International Halocarbons in Air Comparison Experiment (IHALACE), Atmos. Meas. Tech., 7(2), 469-490, doi:10.5194/amt-7-469-2014, 2014.

Ishijima, K., Sugawara, S., Kawamura, K., Hashida, G., Morimoto, S., Murayama, S., Aoki, S., and Nakazawa, T.: Temporal variations of the atmospheric nitrous oxide concentration and its δ 15 N and δ 18 O for the latter half of the 20th century reconstructed from firn air analyses. J. Geophys. Res.-Atmos., 112(D3), 2007.

Jiang, X., Ku, W. L., Shia, R.-L., Li, Q., Elkins, J. W., Prinn, R. G., and Yung, Y. L.: Seasonal cycle of N2O: Analysis of data, Global Biogeochem. Cy., 21, GB1006, doi:10.1029/2006GB002691, 2007.

Khalil, M. A. K., and Rasmussen, R. A.: Increase and seasonal cycles of nitrous oxide in the earth's atmosphere. Tellus, 35B, 161-169, 1983.

Khalil, M. A. K., Rasmussen, R. A., and Shearer, M. J.: Atmospheric nitrous oxide: patterns of global change during recent decades and centuries, Chemosphere, 47, 807–821, 2002.

Kovács, T., Feng, W., Totterdill, A., Plane, J. M. C., Dhomse, S., Gómez-Martín, J. C., Stiller, G. P., Haenel, F. J., Smith, C., Forster, P. M., García, R. R., Marsh, D. R., and Chipperfield, M. P.: Determination of the atmospheric lifetime and global warming potential of sulfur hexafluoride using a three-dimensional model, Atmos. Chem. Phys., 17, 883-898, https://doi.org/10.5194/acp-17-883-2017, 2017.

Levin, I. and Hesshaimer, V.: Refining of atmospheric transport model entries by the globally observed passive tracer distributions of 85krypton and sulfur hexafluoride (SF6), J. Geophys. Res.-Atmos., 101(D11), 16745-16755, doi:10.1029/96JD01058, 1996.

Levin, I., Naegler, T., Heinz, R., Osusko, D.,Cuevas, E., Engel A., Ilmberger, J., R. Langenfelds, R. L., Neininger, B., Rohden, C. v., Steele, L. P., Weller, R., Worthy, D. E., and Zimo, S. A.: The global SF6 source inferred from long-term high precision atmospheric measurements and its comparison with emission inventories, Atmos. Chem. and Phys., 10, 2655–2662, 2010.

Liao, T., Camp, C., and Yung, Y.: The seasonal cycle of N2O, Geophys. Res. Lett., 31, L17108, doi:10.1029/2004GL020345, 2004.

Liang, Q., Stolarski, R., Douglass, A., Newman, P., and Nielsen, J.: Evaluation of emissions and transport of CFCs using surface observations and their seasonal cycles and the GEOS CCM simulation with emissions-based forcing. J. Geophys. Res.-Atmos., 113(D14), doi:10.1029/2007JD009617, 2008.

Lueker, T., Walker, S., Vollmer, M., Keeling, R., Nevison, C., Weiss, R., and Garcia, H: Coastal upwelling air-sea fluxes revealed in atmospheric observations of O2/N2, CO2, and N2O, Geophys. Res. Lett., 30(6), 1292, doi:10.1029/2002GL016615, 2003.

Maiss, M. and Brenninkmeijer, C.: Atmospheric SF6: Trends, sources, and prospects, Environ. Sci. Technol., 32(20), 3077–3086, 1998.

Maiss, M., Steele, L. P., Francey, R., Fraser, P., Langenfelds, R., Trivett, N., and Levin, I.: Sulfur hexafluoride – a powerful new atmospheric tracer, Atmos. Environ., 30(10), 1621–1629, doi:10.1016/1352-2310(95)00425-4, 1996.

Meinshausen, M., Vogel, E., Nauels, A., Lorbacher, K., Meinshausen, N., Etheridge, D. M., Fraser, P. J., Montzka, S. A., Rayner, P. J., Trudinger, C. M., Krummel, P. B., Beyerle, U., Canadell, J. G., Daniel, J. S., Enting, I. G., Law, R. M., Lunder, C. R., O'Doherty, S., Prinn, R. G., Reimann, S., Rubino, M., Velders, G. J. M., Vollmer, M. K., Wang, R. H. J., and Weiss, R.: Historical greenhouse gas concentrations for climate modelling (CMIP6). Geosci. Model Dev., 10(5), 2057-2116, 2017.

Myhre, G., Shindell, D., Bréon, F.-M., Collins, W., Fuglestvedt, J., Huang, J., Koch, D., Lamarque, J.-F., Lee, D., Mendoza, B., Nakajima, T., Robock, A., Stephens, G., Takemura, T., and Zhang, H.: Anthropogenic and Natural Radiative Forcing. In: Climate Change 2013: The Physical Science Basis. Contribution of Working Group I to the Fifth Assessment Report of the Intergovernmental Panel on Climate Change [Stocker, T.F., Qin, D., Plattner, G.-K., Tignor, M., Allen, S.K., Boschung, J., Nauels, A., Xia, Y., Bex, V., and Midgley, P.M. (eds.)]. Cambridge University Press, Cambridge, United Kingdom and New York, NY, USA, 2013.

Nevison, C., Kinninson, D., and Weiss, R.: Stratospheric influences on the tropospheric seasonal cycles of nitrous oxide and chlorofluorocarbons, Geophys. Res. Lett., 31(20), doi:10.1029/2004GL020398, 2004.

Nevison, C., Mahowald, N., Weiss, R., and Prinn, R.: Interannual and seasonal variability in atmospheric N2O, Global Biogeochem. Cy., 21(3), doi:10.1029/2006GB002755, 2007.

Olivier, J., Van Aardenne, J., Dentener, F., Pagliari, V., Ganzeveld, L., and Peters, J.: Recent trends in global greenhouse gas emissions:regional trends 1970–2000 and spatial distribution of key sources in 2000, Environ. Sci., 2(2-3), 81-99, doi:10.1080/15693430500400345, 2005.

Park, S., Croteau, P. Boering, K. A., Etheridge, D. M., Ferretti, D., Fraser, P. J., Kim, K-R., Krummel, P. B., Langenfelds, R. L., van Ommen, T. D., Steele, L. P., Trudinger, C. M.: Trends and seasonal cycles in the isotopic composition of nitrous oxide since 1940, Nat. Geosci., 5(4), 261-265, doi:10.1038/NGEO1421, 2012.

Patra, P. K., Takigawa, M., Dutton, G. S., Uhse, K., Ishijima, K., Lintner, B. R., Miyazaki, K., and Elkins, J. W.: Transport mechanisms for synoptic, seasonal and interannual SF6 variations and "age" of air in troposphere, Atmos. Chem. and Phys., 9, 1209–1225, 2009.

Prather, M. J., Holmes, C. D., and J. Hsu, J.: Reactive green house gas scenarios: Systematic exploration of uncertainties and the role of atmospheric chemistry, Geophys. Res. Lett., 39, L09803, doi:10.1029/2012GL051440, 2012.

Prather, M. J., Hsu, J., DeLuca, N. M., Jackman, C. H., Oman, L. D., Douglass, A. R., Fleming, E. L., Strahan, S. E., Steenrod, S. D., Søvde, O. A., Isaksen, I. S. A., Froidevaux, L., and Funke, B.: Measuring and modeling the lifetime of nitrous oxide including its variability, J. Geophys. Res.-Atmos., 120(11), 5693-5705, doi:10.1002/2015JD023267, 2015.

Prinn, R., Cunnold, D., Rasmussen, R., Simmonds, P., Alyea, F., Crawford, A., Fraser, P., and Rosen, R.: Atmospheric emissions and trends of nitrous oxide deduced from 10 years of ALE-GAGE data, J. Geophys. Res., 95(D11), 18369-18385, 1990.

Prinn, R., Weiss, R., Fraser, P., Simmonds, P., Cunnold, D., Alyea, F., O'Doherty, S., Salameh, P., Miller, B. R., Huang, J., Wang, R. H. J., Hartley, D. E., Harth, C., Steele, L. P., Sturrock, G., Midgley, P. M., and McCulloch, A.: A history of chemically and radiatively important gases in air deducted from ALE/GAGE/AGAGE, J. Geophys. Res., 105(D14), 17751-17792, doi:10.1029/2000JD900141, 2000.

Prinn, R. G., Weiss, R. F., Arduini, J., Arnold, T., Dewitt, H. L., Fraser, P. J., Ganesan, A. L., Gasore, J., Harth, C. M., Hermansen, O., Kim, J., Krummel, P. B., Li, S., Loh, Z. M., Lunder, C. R., Maione, M., Manning, A. J., Miller, B. R., Mitrevski, B., Mühle, J., O'Doherty, S., Park, S., Reimann, S., Rigby, M., Saito, T., Salameh, P. K., Schmidt, R., Simmonds, P. G., Steele, L. P., Vollmer, M. K., Wang, R. H., Yao, B., Yokouchi, Y., Young, D., and Zhou, L.: History of Chemically and Radiatively Important Atmospheric Gases from the Advanced Global Atmospheric Gases Experiment (AGAGE). Earth Syst. Sci. Data, 10.2, 985-1018, 2018.

Ray, E., Moore, F. L., Elkins, J. W., Rosenlof, K. H., Laube, J. C., Röckmann, T., Marsh, D. R., and Andrews. A. E.: Quantification of the SF6 Lifetime Based on Mesospheric Loss Measured in the Stratospheric Polar Vortex, J. Geophys. Res.-Atmos., 122(8), 4626-4638, doi:10.1002/2016JD026198, 2017.

~~Ravishankara, A., Solomon, S., Turnipseed, A., and Warren, R.: The atmospheric lifetimes of long-lived halogenated species, Science, 259, 194–199, 1993.~~

Rice, A. L., Butenhoff, C. L., Teama, D. G., Röger, F. H., M. Khalil, M. A. K., and Rasmussen, R. A.: Atmospheric methane isotopic record favors fossil sources flat in 1980s and 1990s with recent increase, P. Natl. Acad. Sci. USA, 113(39), 10791-10796, 2016.

Rigby, M., Muhle, J., Miller, B. R., Prinn, R. G., Krummel, P. B., Steele, L. P., Fraser, P. J., Salameh, P. K., Harth, C. M., Weiss, R. F., Greally, B. R., O'Doherty, S., Simmonds, P. G., Vollmer, M. K., Reimann, S., Kim, J., Kim, K.-R., Wang, H. J., Olivier, J. G. J., Dlugokencky, E. J., Dutton, G. S., Hall, B. D., and Elkins, J. W.: History of atmospheric SF6 from 1973 to 2008, Atmos. Chem. and Phys., 10, 10305–10320, 2010.

Saikawa, E., Prinn, R. G., Dlugokencky, E., Ishijima, K., Dutton, G. S.,Hall, B. D., Langenfelds, R., Tohjima, Y., Machida, T., Manizza, M., Rigby, M., O'Doherty, S., Patra, P. K., Harth, C. M., Weiss, R. F., Krummel, P. B., van der Schoot, M., Fraser, P. J., Steele, L. P., Aoki, S., Nakazawa, T., and Elkins, J. W.: Global and regional emissions estimates for N2O, Atmos., Chem., and Phys., 14, 4617–4641, 2014.

Schmidt, M., Glatzel-Mattheier, H., Sartorius, H., Worthy, D. E., and Levin, I.: Western European N2O emissions: A top-down approach based on atmospheric observations, J. Geophys. Res., 106(D6), 5507-5515, 2001.

Snider, D. M., Venkiteswaran, J. J., Schiff, S. L., Spoelstra, J.: From the ground up: Global nitrous oxide sources are constrained by stable isotope values, PLOS ONE, 10(3), doi:10.1371/journal.pone.011895, 2015.

Stocker, B. D., Roth, R., Joos, F., Spahni, R., Steinacher, M., Zeahle, S., Bouwman, L., and Prentice, I. C.: Multiple greenhouse-gas feedbacks from the land biosphere under future climate change scenarios, Nat. Clim. Change, 3(7), 666-672, doi:10.1038/nclimate1864, 2013.

Sulfur Hexafluoride (SF_6) WMO Scale: https://www.esrl.noaa.gov/gmd/ccl/sf6_scale.html, last access: 17 June 2018.

Vollmer, M. K., Young, D., Trudinger, C. M., Mühle, J., Henne, S., Rigby, M., Park, S., Li, S., Guillevic, M., Mitrevski, B., Harth, C. M., Miller, B. R., Reimann, S., Yao, B., Steele, L. P., Wyss, S. A., Lunder, C. R., Arduini, J., McCulloch, A., Wu, S., Rhee, T. S., Wang, R. H. J., Salameh, P. K., Hermansen, O., Hill, M., Langenfelds, R. L., Ivy, D., O'Doherty, S., Krummel, P. B., Maione, M., Etheridge, D. M., Zhou, L., Fraser, P. J., Prinn, R. G., Weiss, R. F., and Simmonds, P. G.: Atmospheric histories and emissions of chlorofluorocarbons CFC-13 ($CClF_3$), ΣCFC-114 ($C_2Cl_2F_4$), and CFC-115 (C_2ClF_5), Atmos. Chem. Phys., 18, 979-1002, 2018.

Wilson, C., Chipperfield, M. P., Gloor, M., and Chevallier, F.: Development of a variational flux inversion system (INVICAT v1.0) using the TOMCAT chemical transport model, Geosci. Model Dev., 7(5), 2485-2500, 2014.

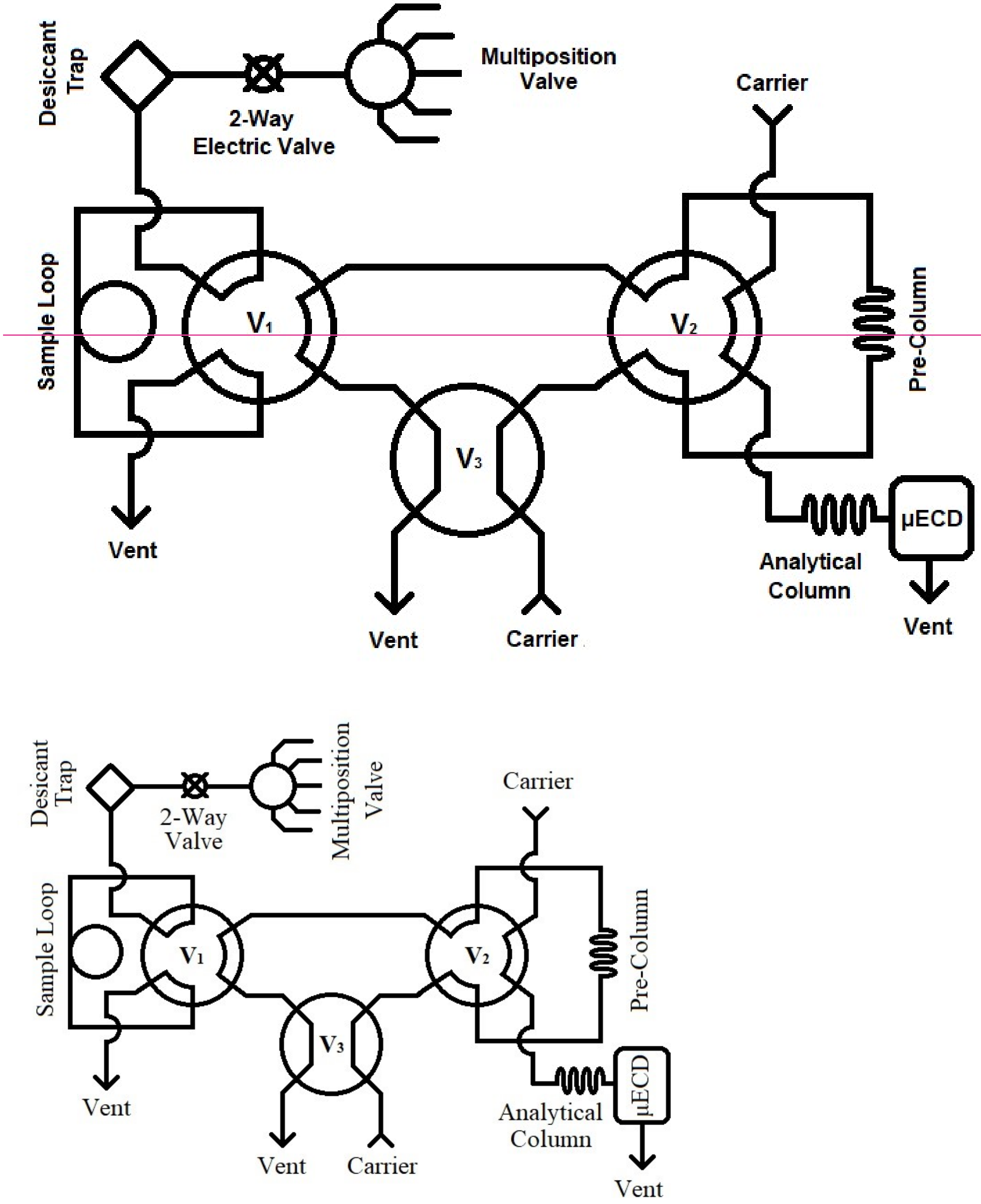

Figure 1. Schematic view of the analytical system for sample evaluation. The system is shown in "back-flush" mode. V_1 = Valve 1, V_2 = Valve 2, V_3 = Valve 3.

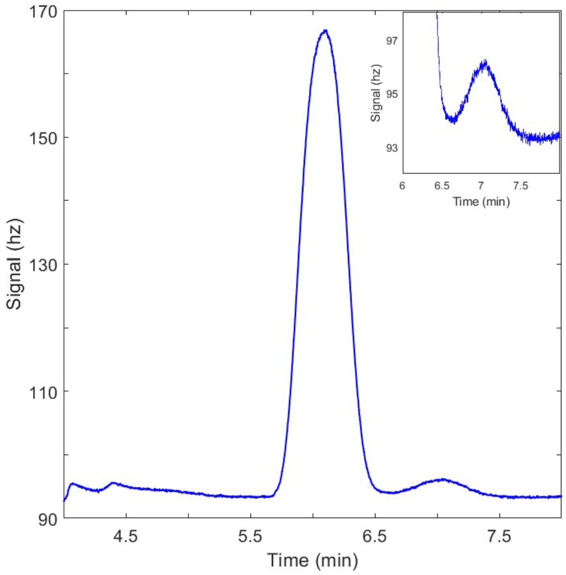

Figure 2. Sample chromatogram showing N_2O peak at a retention time of 6.1 minutes and SF_6 peak at a retention time of 7.0 minutes. Upper-right corner inlay shows an enlarged plot of the SF_6 peak.

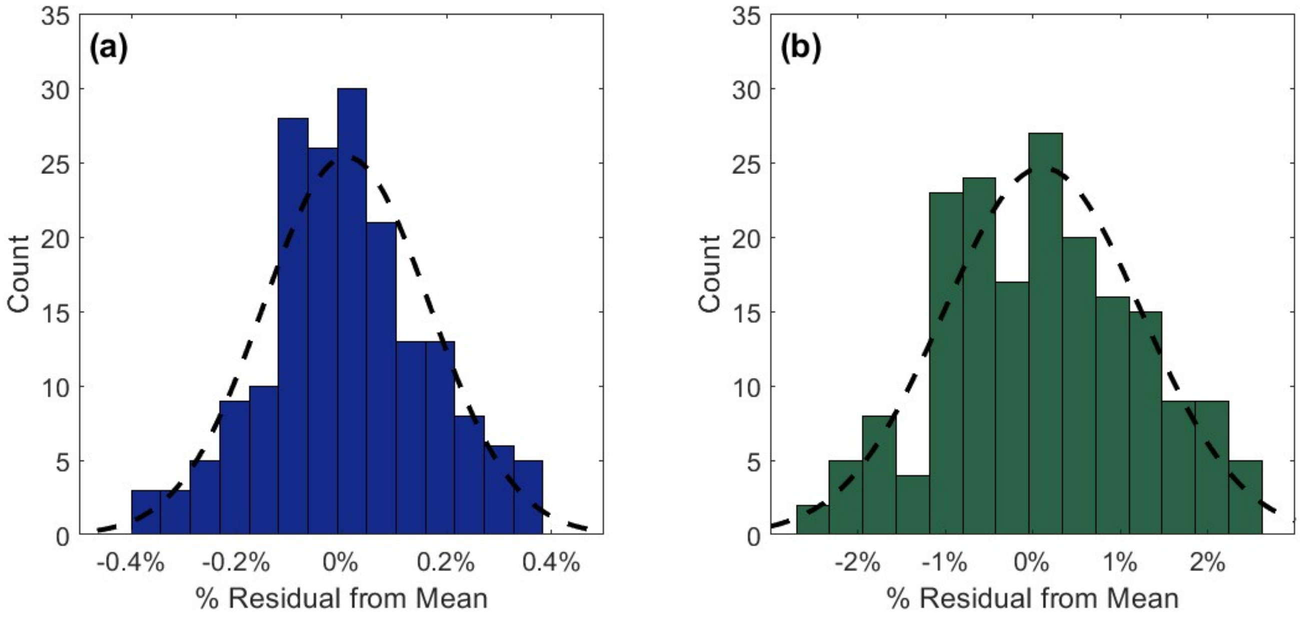

Figure 3. Precision in measurement for N_2O (a) and SF_6 (b) expressed as percent relative standard deviation from 30 sets of 6 measurements of the NOAA reference gas. The black dotted line represents a normal distribution curve with the same mean and standard deviation. The standard deviation for N_2O and SF_6 is 0.16% and 1.1%, respectively.

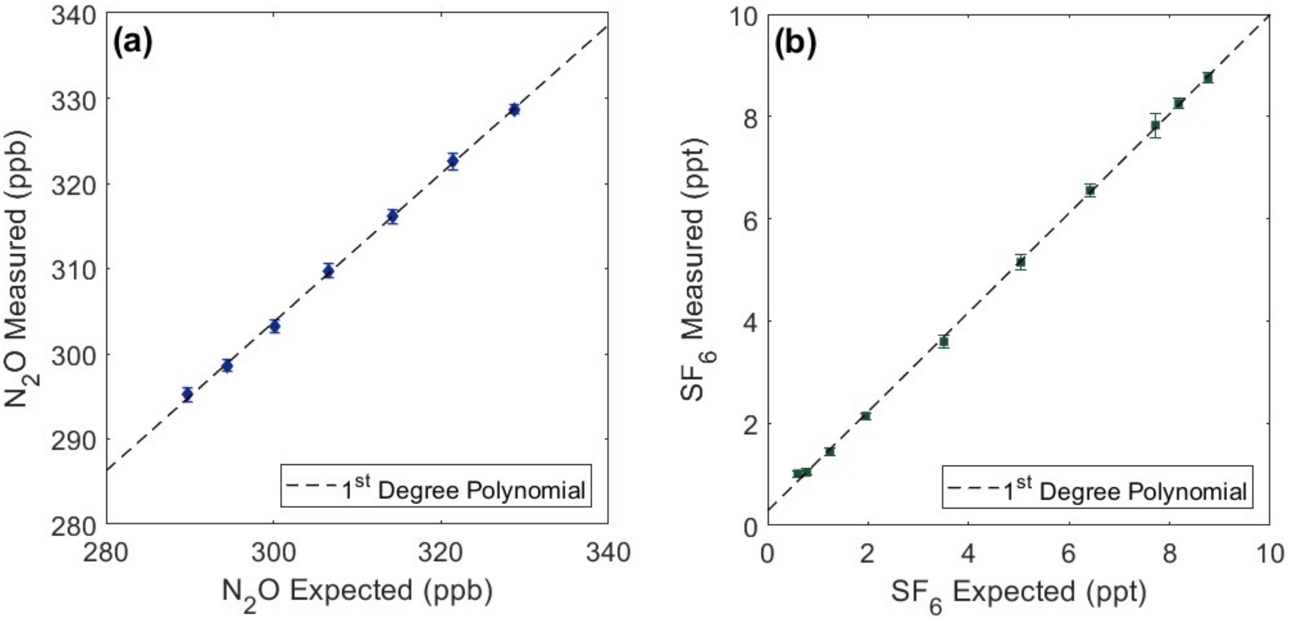

Figure 4. Measurement linearity from plots of measured mole fraction vs. expected mole fraction of N_2O (a) and SF_6 (b). Expected mole fraction is calculated from the NOAA reference mole fraction (328.71 ppb N_2O and 8.76 ppt SF_6) after dilution with ultra-pure air. Error bars represent 1σ total uncertainty.

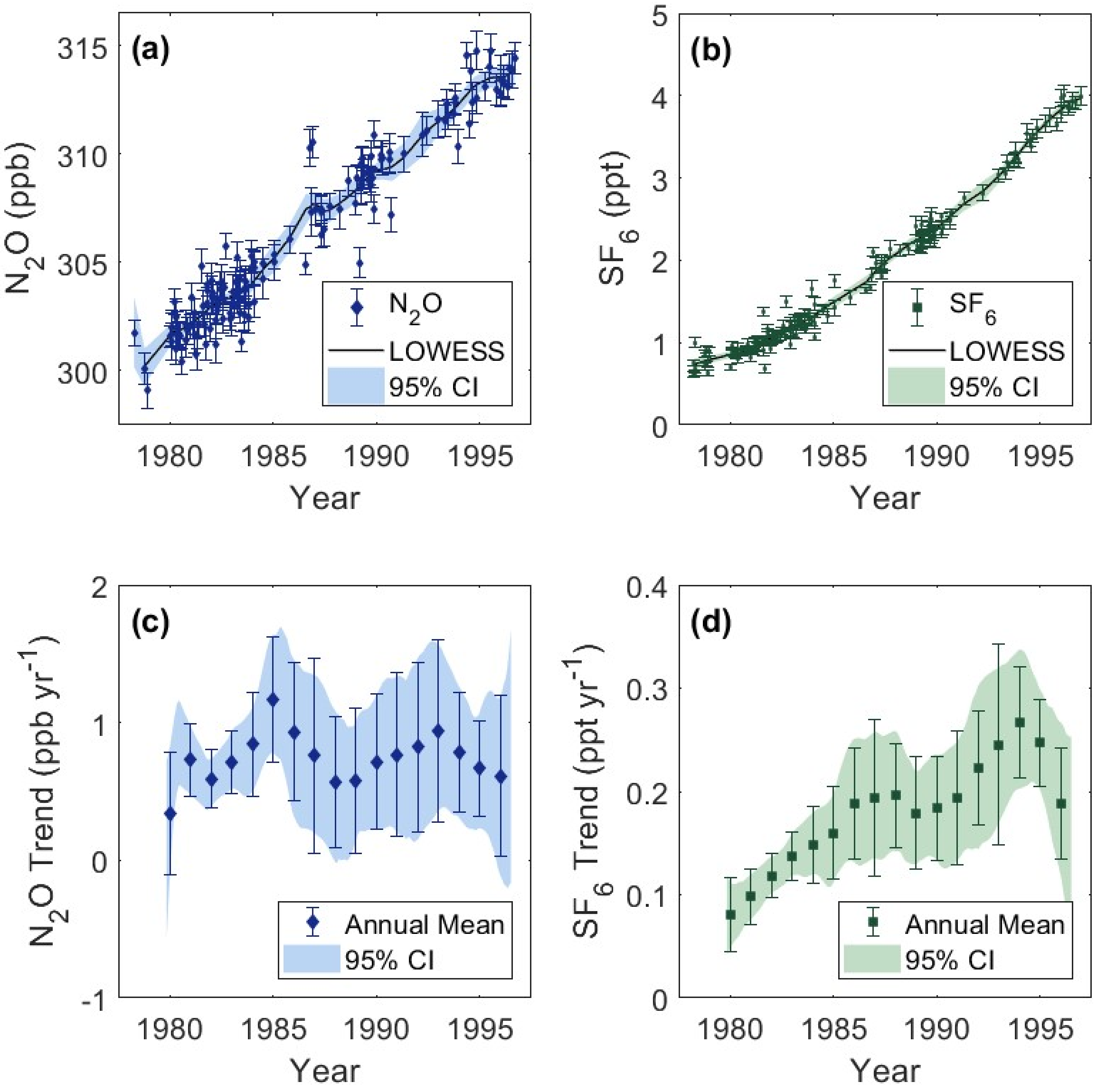

Figure 5. Deseasonalized measurements of mole fraction versus date of collection, N_2O (a) and SF_6 (b), and annual trends in time from Cape Meares, Oregon, N_2O (c) SF_6 (d). Error bars are 1σ uncertainty. The solid black lines are LOWESS fit to the data using a smoothing window of 3 years and shaded areas are 95% confidence intervals in the LOWESS fit calculated from bootstrapping residual variability 1000 times.

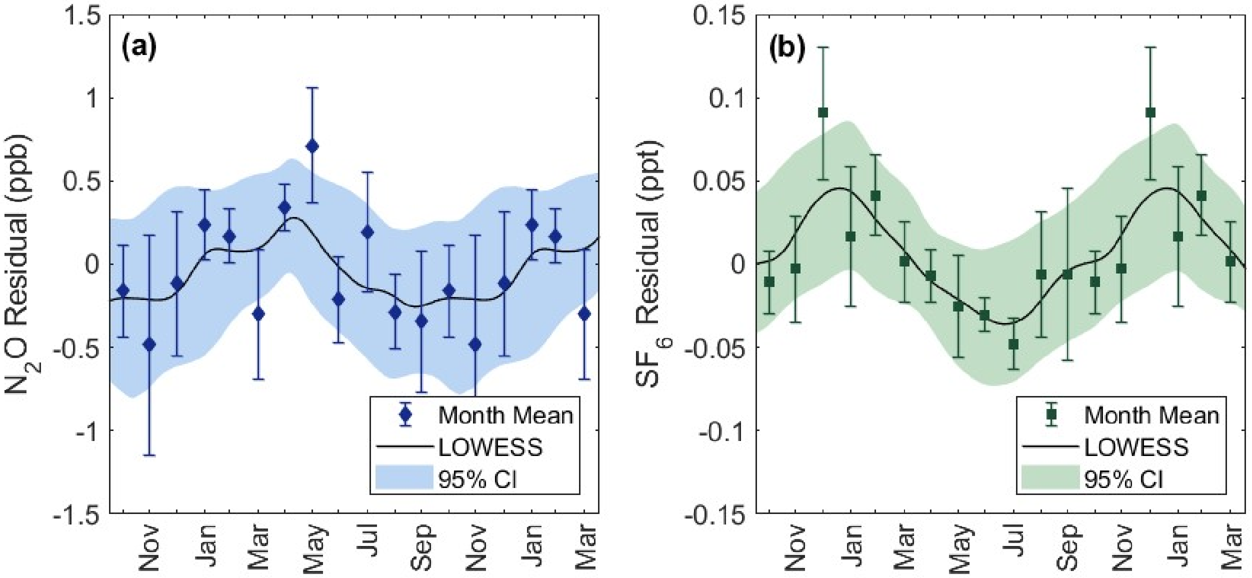

Figure 6. Seasonality for N_2O (a) and SF_6 (b) calculated from the residuals of observed data points to the secular trend. The black line is a LOWESS fit to residuals with a smoothing window of 1 month. Data points show observed monthly mean residual after binning by month with error bars representing standard error within the month. Shaded areas are 95% CI calculated from 1000 bootstrapped LOWESS fits while including the measurement uncertainty to each data point.

Table 1. Characteristics of 12 manometric N_2O dilution samples prepared at Portland State University.

Canister ID	[a] P_{Ref} (kPa)	[b] P_{Total} (kPa)	[c] Expected N_2O Response	[d] Measured N_2O Response	[e] Measured N_2O (ppb)	[f] N_2O 1σ (ppb)
1.7	97.0	132.4	0.7327	0.7673	252.21	0.78
1.14	36.6	132.2	0.2767	0.3262	107.22	0.45
1.5	61.5	132.9	0.4627	0.5157	169.52	0.51
2.14	21.0	132.6	0.1585	0.1941	63.79	0.27
2.7	13.0	132.5	0.0978	0.1239	40.73	0.44
2.5	80.5	132.2	0.6092	0.6535	214.80	0.52
3.7	127.0	132.8	0.9559	0.9618	316.15	0.83
3.5	117.0	132.8	0.8813	0.8981	295.20	0.87
3.14	123.8	132.7	0.9326	0.9423	309.75	0.85
4.5	129.7	132.7	0.9778	0.9813	322.56	0.96
4.14	119.1	132.9	0.8959	0.9085	298.62	0.71
4.7	120.9	132.5	0.9129	0.9226	303.26	0.80

a. P_{Ref} is the NOAA reference gas pressure (in kPa) introduced to the canister.

b. P_{Total} is the final pressure (in kPa) of the canister after balancing with ultra-pure air.

c. Expected response is calculated from the P_{Ref}/P_{Final} fraction.

d. Measured N_2O response of the μECD.

e. Measured N_2O in ppb.

f. N_2O 1σ (ppb) is from combined uncertainty of sample and surrounding NOAA reference.

Table 2. Characteristics of 9 manometric SF_6 dilution samples prepared at Portland State University.

Canister ID	[a] P_{Ref} (kPa)	[b] P_{Scotty} (kPa)	[c] P_{Total} (kPa)	[d] Expected SF_6 Response	[e] Measured SF_6 Response	[f] Measured SF_6 (ppt)	[g] SF_6 1σ (ppt)
1.14	97.0	-	132.4	0.7327	0.7476	6.55	0.12
3.5	117.0	-	132.8	0.8812	0.8943	7.83	0.24
3.14	123.8	-	132.7	0.9326	0.9414	8.25	0.10
1.1	29.6	31.0	132.6	0.2230	0.2443	2.14	0.06
1.18	11.9	36.9	133.0	0.0896	0.1199	1.05	0.07
1.28	8.9	37.6	132.3	0.0674	0.1153	1.01	0.06
2.1	18.7	34.8	131.9	0.1418	0.1644	1.44	0.08
2.18	75.9	16.0	132.2	0.5740	0.5879	5.15	0.15
2.28	52.9	23.5	132.1	0.4002	0.4110	3.60	0.12

a. P_{Ref} is the NOAA reference gas pressure (in kPa) introduced to the canister.

b. P_{Scott} is the 1 ppm N_2O balanced with He (in kPa) introduced to the canister.

c. P_{Total} is the final pressure (in kPa) of the canister after balancing with ultra-pure air.

d. Expected SF_6 response is calculated from the P_{Ref}/P_{Final} fraction.

e. Measured SF_6 response of the μECD.

f. Measured SF_6 in ppt.

g. SF_6 1σ (ppt) is from combined uncertainty of sample and surrounding NOAA reference.